Hanson et al; Supporting Information

Table of contents

Simulation of potential spore yield in colonies with different switching systems

S. cerevisiae and *S. pombe* switch mating types by destroying and replacing the active *MAT* locus, whereas the methylotrophs make a reciprocal swap between the active and silent loci. More specifically, *S. cerevisiae* and *S. pombe* use synthesis-dependent strand annealing (SDSA) to copy information unidirectionally from a silent locus into the broken *MAT* locus. SDSA involves two strand-exchange events, one in each of the homologous guide regions that flank the non-homologous Yalpha and Y**a** regions, and is resolved without crossover (1). These species achieve highly productive switching though biased choice of the appropriate donor; about 80-90% of the cells that are expected to switch do switch correctly to the opposite mating type (2, 3). In contrast, switching in the methylotrophs must preserve the outgoing *MAT* sequence for future re-use and probably proceeds via a single Holliday junction in the IR. This difference makes it unlikely that the methylotrophs can achieve the same levels of productive switching as *S. cerevisiae* and *S. pombe*, because the Holliday junction is expected to be resolved randomly into crossover (inverted) and non-crossover molecules (4), leading to a maximum of 50% successful switching from each attempt.

We used computer simulation (Fig. 6; Fig. S9) to study how efficiently different switching systems enable a small colony to make new spores if the environment demands it. Cells were followed in 10,000 replicate colonies, each starting from a single *MAT*alpha spore and going through 7 mitotic divisions to the 128-cell stage. At each cell division, probabilistic rules for switching were applied corresponding to each known system (Fig. S9). All switching systems cause the frequency of the founder *MAT*alpha allele to decline towards 50% (Fig. 6). In the *S. cerevisiae* and *S. pombe* systems, changing the productivity of switching from 50% (no donor bias) to 90% (strong donor bias) causes the frequency of *MAT*alpha to decline faster. In the methylotroph system, the founder allele frequency falls quickly if switching is 50% productive, and more slowly if it is only 10% productive.

The ability of a simulated colony to make new spores was measured as the 'potential spore yield', defined as *S/Smax* where *S* is the number of spores that would be made if all pairs of cells in the colony with opposite mating types mated and sporulated, and *Smax* is the number that would be made if mating type did not matter and any two cells could mate. Potential spore yield is reduced by unequal allele frequencies, leaving some cells without a partner (5). In all systems except *P. pastoris*, it is simply twice the frequency of the rarer *MAT* allele (Fig. 6). Donor bias greatly increases potential spore yield relative to unbiased switching, especially at the 4-32 cell stages in *S. cerevisiae* and the 8-16 cell stages in *S. pombe*. Yield in *H. polymorpha* is low if it switches with 10% productivity, but at 50% productivity its yield is identical to that of *S. cerevisiae* in the absence of donor bias. As argued above we do not think that the productivity of switching in *H. polymorpha* can exceed 50%, but even if it does, potential spore yield declines again (the curves for 10% and 90% productivity are identical).

We simulated *P. pastoris* under the assumption that meiotic recombination can occur in the 123-kb unique region between the inner IRs, and that the genetic length of this region is 50 centimorgans, which leads to 2 inviable spores per meiosis. Thus potential spore yield in the *P. pastoris* model is low relative to *H. polymorpha*, for which we assumed no meiotic recombination in the 19-kb region. However, if inversion at the inner IRs of *P. pastoris* is permitted, yield increases (Fig 6).

Supplementary Figure Legends

Fig. S1. RT-PCR showing expression of genes between *MAT* loci within the 19-kb invertible region in *H. polymorpha*. Amplified cDNA was generated from haploid strains of **a** or alpha orientation. SH4331 is derived from NCYC495 background. +/- RT indicates addition of reverse transcriptase to the cDNA synthesis reaction.

Fig. S2. Localization of *H. polymorpha* centromeres by reanalysis of Hi-C data (6).
(*A*) Hi-C chromosomal contact matrix. Dots show single (green) and multiple (yellow) interactions, in 10 kb windows. Signals at consistent positions in each inter-chromosomal comparison derive from physical interactions between the centromeres of different chromosomes.
(*B*) Local interaction intensity on NCYC495 chromosome 3 shows a peak at 897 kb. LTRs of the Ty5-like retrotransposon Tpa5 are marked by orange circles. The red box shows the region magnified in D.
(*C*) G+C content variation (7) on chromosome 3.
(*D*) Expressed sequence tag coverage (blue) of the region between 875-975 kb on chromosome 3, showing that centromere is transcriptionally silent. The graphic below shows a complete Tpa5 retrotransposon (brown) in the centromeric region, the two IRs (gray) at 900 and 921 kb, *MAT*a genes (green), *MAT*alpha genes (purple), and other annotated genes (orange). The EST data was generated by the Joint Genome Institute (NCBI SRR346565) and mapped onto a version of the NCYC495 genome that was converted bioinformatically to the alpha orientation because the *MAT*alpha genes are more strongly expressed in the EST data.

Fig. S3. RT-PCR showing expression of all four *MAT* genes in *P. pastoris* haploids with both orientations of the 138-kb region, and in diploids. Amplified cDNA was generated from haploid and diploid strains representing all four possible *MAT* locus organizations (alpha+, alpha-, **a**+, **a**-). +/- RT indicates addition of reverse transcriptase to cDNA synthesis reaction.

Fig. S4. Southern blot showing *MAT* locus orientation in *P. pastoris* strains GS115 and GS190. Schematics show location of restriction sites and probes (dark purple bars) used in the blot to determine orientation of *(A)* the outer inverted repeats, shown as blue rectangles, and *(B)* the inner inverted repeats shown as purple rectangles. Magenta and green regions represent *MAT*alpha and *MAT*a regions, respectively. Letters A and G correspond to primer locations used in PCRs in Figure 5. The orange circle the telomere. DNA was extracted from haploid strains grown in YPD or minimal (NaKG) medium for 0 or 4 hours. Hybridization reactions were performed with random-primed digoxigenin-labeled probes (Roche) generated according to manufacturer's instructions.

Fig. S5. Scale map of *MAT* locus regions in *H. polymorpha* and *P. pastoris*. Inverted repeat regions are highlighted in purple and blue. Numbers below the *MAT* genes are the percentage amino acid sequence identities to their *K. lactis* orthologs in a ClustalW alignment.

Fig. S6. Consequences of meiotic recombination between oppositely-oriented *MAT* regions in *P. pastoris*. The upper panel represents a diploid genome entering meiosis I with replicated copies of chromosome 4 in alpha- and **a**+ orientations. If a meiotic recombination occurs within the 123-kb invertible region (orange arrow), chromosomes with large duplications and deficiencies will be produced, probably making two of the four spores inviable. If the centromere is located in the 1.7 Mb region, the recombinant chromosomes will also be dicentric and acentric. A general conclusion is that the larger the invertible region, the higher the probability of recombination within it, and hence the higher the expected number of inviable spores. If the two ends of the invertible region are so far apart that they are genetically unlinked, the fraction of recombinant chromosomes is expected to be 50%, and the average number of viable spores per meiosis will be 2 (as simulated in model Ppas_50/0 in Fig. 6). Alternatively (for example), if the two ends of the invertible segment are only 10 centimorgans apart the average number of viable spores per meiosis will be 3.6.

Fig. S7. Model for the origin of a flip-flop inversion system by introgression between *MAT* idiomorphs in a heterothallic species, based on the model of Chitrampalam *et al.* (8) for *Sclerotinia sclerotiorum.* The three chromosome rearrangement events shown could all involve recombination at short sequence repeats.

Fig. S8. Sequence of *H. polymorpha* tagged *CSE4* construct.

Fig. S9. Models of cell lineages during mating-type switching in different yeast species, and computational framework for simulations. Panels *A*-*C* show DNA replication and cell division events from a single haploid cell (spore) to the 8-cell stage in 3 switching systems. Red arrows indicate steps in which switching is permitted, and black asterisks indicate cells that are competent to switch. The frequency of productive switching, *f*, is the probability that a cell that attempts to switch succeeds in changing its mating type.
(*A*) *S. cerevisiae* model using the nomenclature of Herskowitz (5). Cells are mating type alpha (green/magenta DNA strands) or **a** (blue DNA strands). Only mother cells can switch, and switched cells appear in pairs because switching occurs prior to S phase. If switching is fully productive, 2/4 grandchildren and 4/8 great-grandchildren of the original cell will show a switched mating type. In practice, switching is about 90% productive (f = 0.9). We also simulated *S. cerevisiae* switching without donor bias (f = 0.5).
(*B*) *S. pombe* strand-segregation model using the nomenclature of Klar (2). Cells are mating type P or M, and are either switchable (s) or unswitchable (u). Green and magenta indicate the Watson and Crick DNA strands of a P allele at the *mat1* locus, and blue indicates an M allele. Arrowheads on DNA strands indicate new synthesis. An origin of replication is located to the right of the *mat1* locus as drawn, so the Watson strand is always synthesized as a lagging strand. A switchable cell is one that contains two ribonucleotides (green asterisk) at a specific site in the Watson strand, left behind by incomplete removal of an RNA primer during lagging strand synthesis. When the cell attempts to use this imprinted strand as a template for DNA synthesis, replication fails and a double-strand break is formed, leading to mating type switching. If switching is fully productive, 1/4 grandchildren and 4/8 great-grandchildren of the original cell will show a switched mating type. In practice, switching is about 90% productive (f = 0.9). We also simulated *S. pombe* switching without donor bias (f = 0.5).

(*C*) Model for *H. polymorpha* and other species that use a 2-locus inversion system. Cells are mating type alpha or **a**. All cells can switch. Switched cells appear in pairs because switching occurs prior to S phase. Switching is maximally 50% productive (*f* = 0.5) because no more than 50% of Holliday junctions in the IR can be resolved as crossovers. Unlike the *S. pombe* and *S. cerevisiae* models, which are essentially deterministic because of their high productivity, the *H. polymorpha* model is probabilistic so different 8-cell colonies will contain different numbers of alpha and **a** cells. The example shown is one of many possible outcomes, depending on whether each cell that is competent to switch actually switches. We simulated *H. polymorpha* with all cells attempting to switch (*f* = 0.5), and with 20% of cells attempting to switch (*f* = 0.1). The model for *P. pastoris* is identical to *H. polymorpha* except that we tracked orientation of the 123-kb unique region and modeled inversion by recombination in the inner IR at either 0% or 10% probability (Fig. 5).
(*D*) Generic framework for computer simulations of switching. Cells have a mating type (1 or 0) and are switchable (s) or unswitchable (u). *P0* is the probability of switching mating type (from 1 to 0 or vice versa) in a parental cell prior to DNA replication, which will cause switched cells to appear in pairs. *P1* and *P2* are probabilities of a switch occurring in progeny 1 or progeny 2 after DNA replication. The probabilities *P0*, *P1*, and *P2* are either zero or *f*, depending on the species being modeled, as shown in the Table, where *f* is the expected average frequency of productive switching in cells that are competent to switch. There are no unswitchable cells in the *H. polymorpha* model. In *S. cerevisiae*, progeny 1 and 2 correspond to mother and daughter cells, respectively. Genotypes under this generic framework are shown at the bottom of panels *A*-*C*. Our simulations started with a single cell in state 1u (or 1s for *H. polymorpha*) and followed cell divisions for 7 generations with *P0, P1* and *P2* as specified, for various values of *f* (0.1, 0.5, 0.9), in 10,000 replicate colonies for each set of parameters.

References for SI Appendix.

1. Haber JE, Ira G, Malkova A, Sugawara N (2004) Repairing a double-strand chromosome break by homologous recombination: revisiting Robin Holliday's model. *Philos Trans R Soc Lond B Biol Sci* 359: 79-86.
2. Klar AJ (2007) Lessons learned from studies of fission yeast mating-type switching and silencing. *Annu Rev Genet* 41: 213-236.
3. Strathern JN, Herskowitz I (1979) Asymmetry and directionality in production of new cell types during clonal growth: the switching pattern of homothallic yeast. *Cell* 17: 371-381.
4. Klein HL, Symington LS (2012) Sgs1--the maestro of recombination. *Cell* 149: 257-259.
5. Herskowitz I (1988) Life cycle of the budding yeast *Saccharomyces cerevisiae*. *Microbiol Rev* 52: 536-553.
6. Burton JN, Liachko I, Dunham MJ, Shendure J (2014) Species-level deconvolution of metagenome assemblies with Hi-C-based contact probability maps. *G3 (Bethesda)* 4: 1339-1346.
7. Lynch DB, Logue ME, Butler G, Wolfe KH (2010) Chromosomal G + C content evolution in yeasts: systematic interspecies differences, and GC-poor troughs at centromeres. *Genome Biol Evol* 2: 572-583.
8. Chitrampalam P, Inderbitzin P, Maruthachalam K, Wu BM, Subbarao KV (2013) The *Sclerotinia sclerotiorum* mating type locus (*MAT*) contains a 3.6-kb region that is inverted in every meiotic generation. *PLoS One* 8: e56895.

Hanson et al; Fig. S1

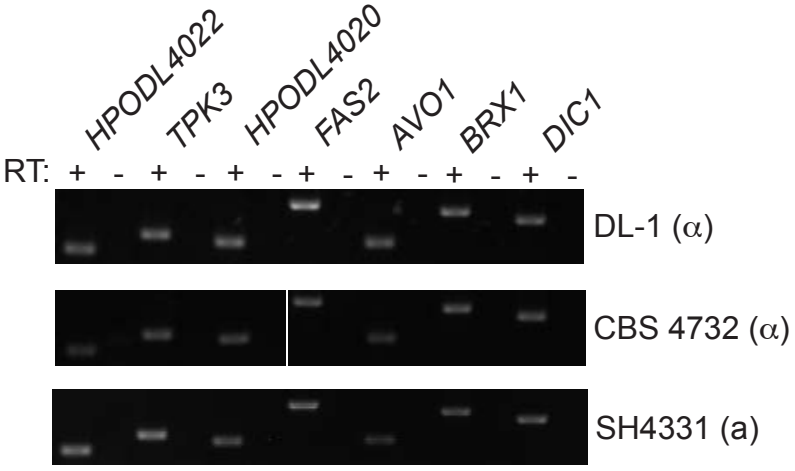

Hanson et al; Fig. S2

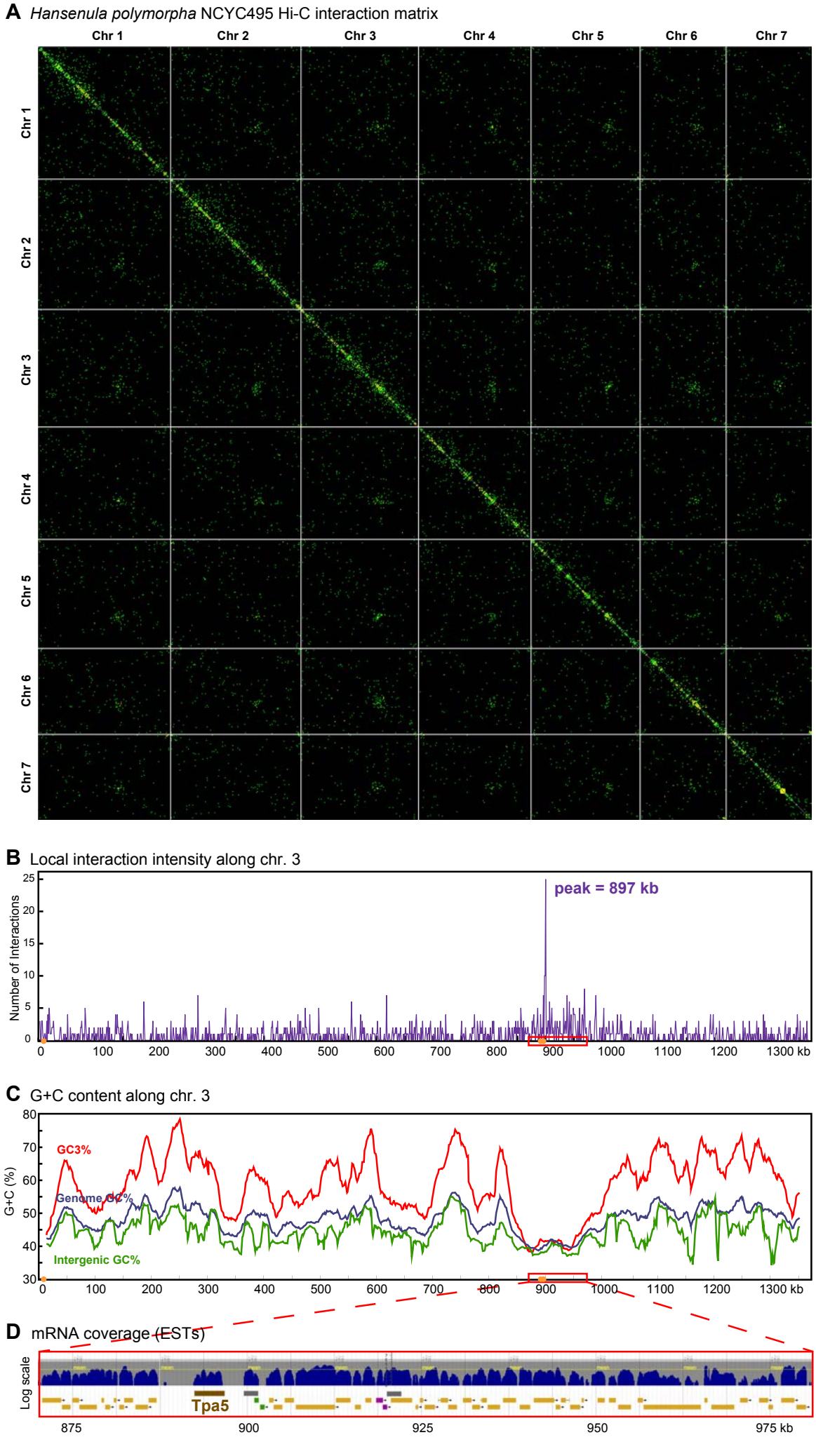

Hanson et al; Fig. S3

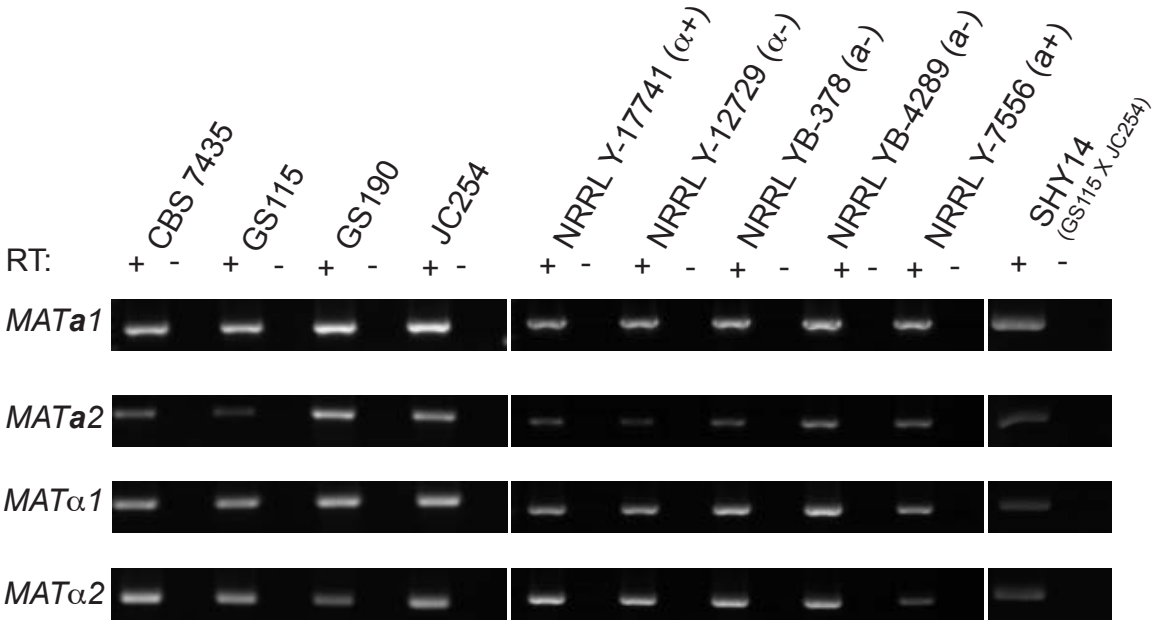

Hanson et al; Fig. S4

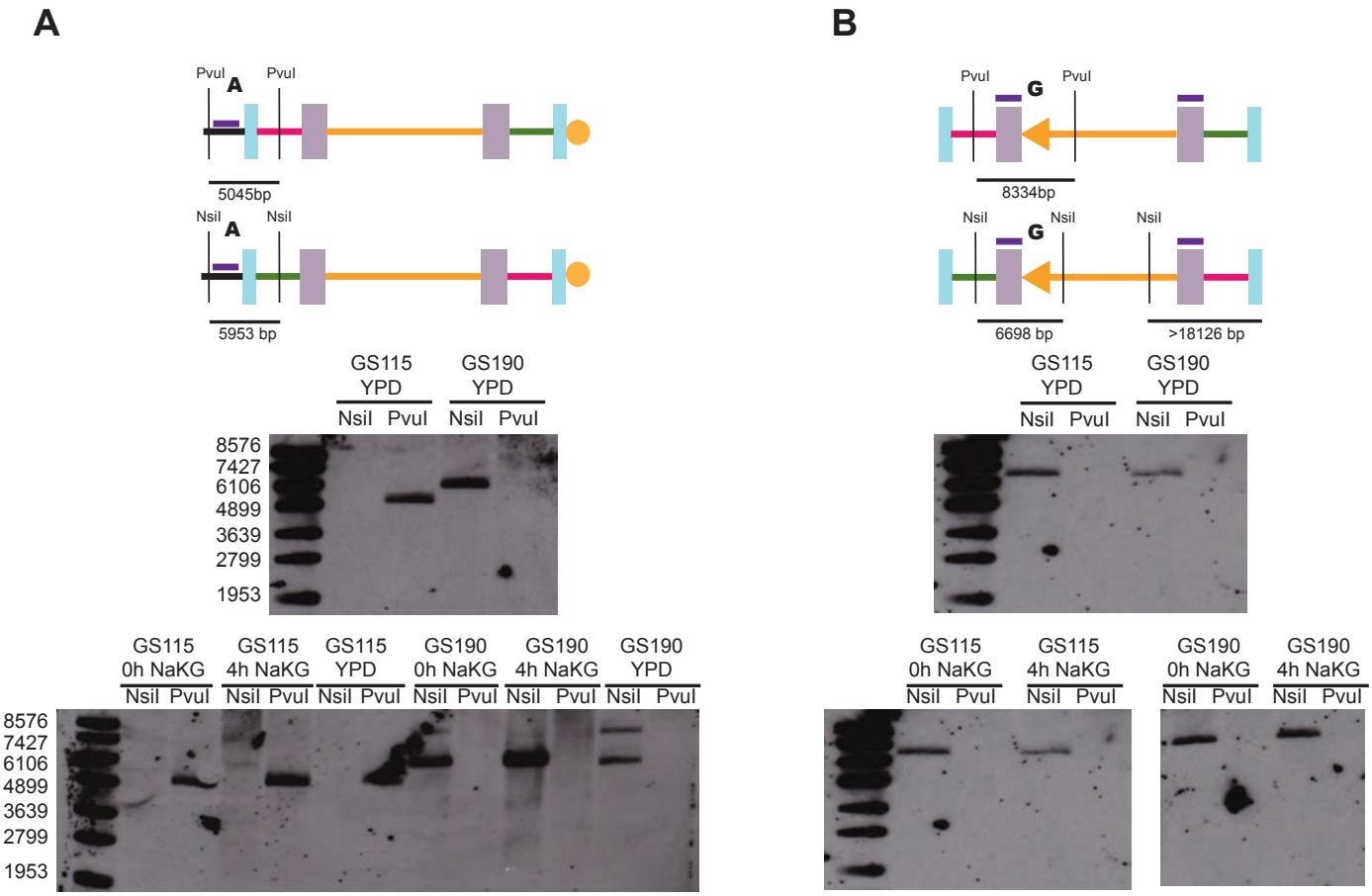

Hanson et al; Fig. S5

Hansenula polymorpha (NCYC495 chromosome 3 in **a** orientation; http://genome.jgi.doe.gov/Hanpo2/Hanpo2.home.html)

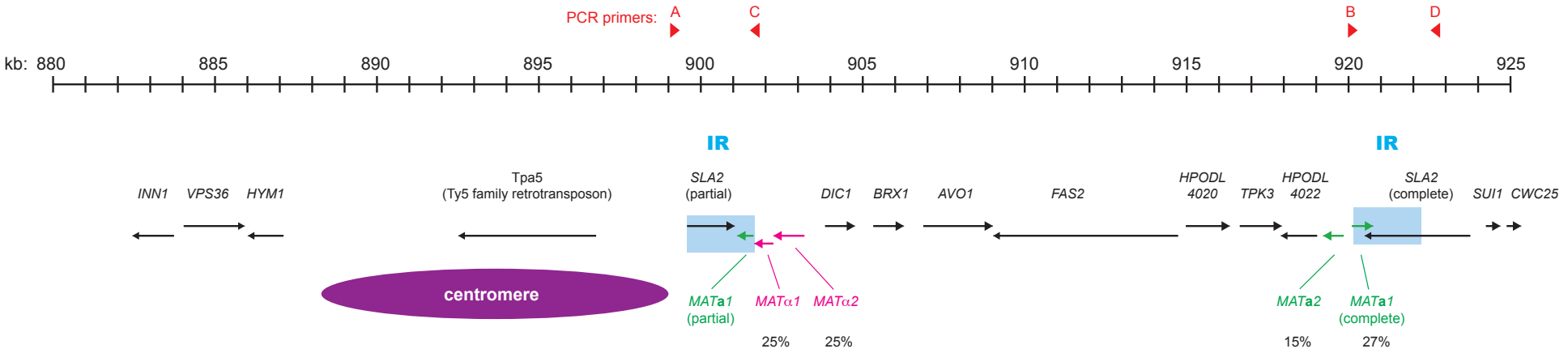

Pichia pastoris (CBS7435 chromosome 4 in **alpha+** orientation GenBank FR839631.1)

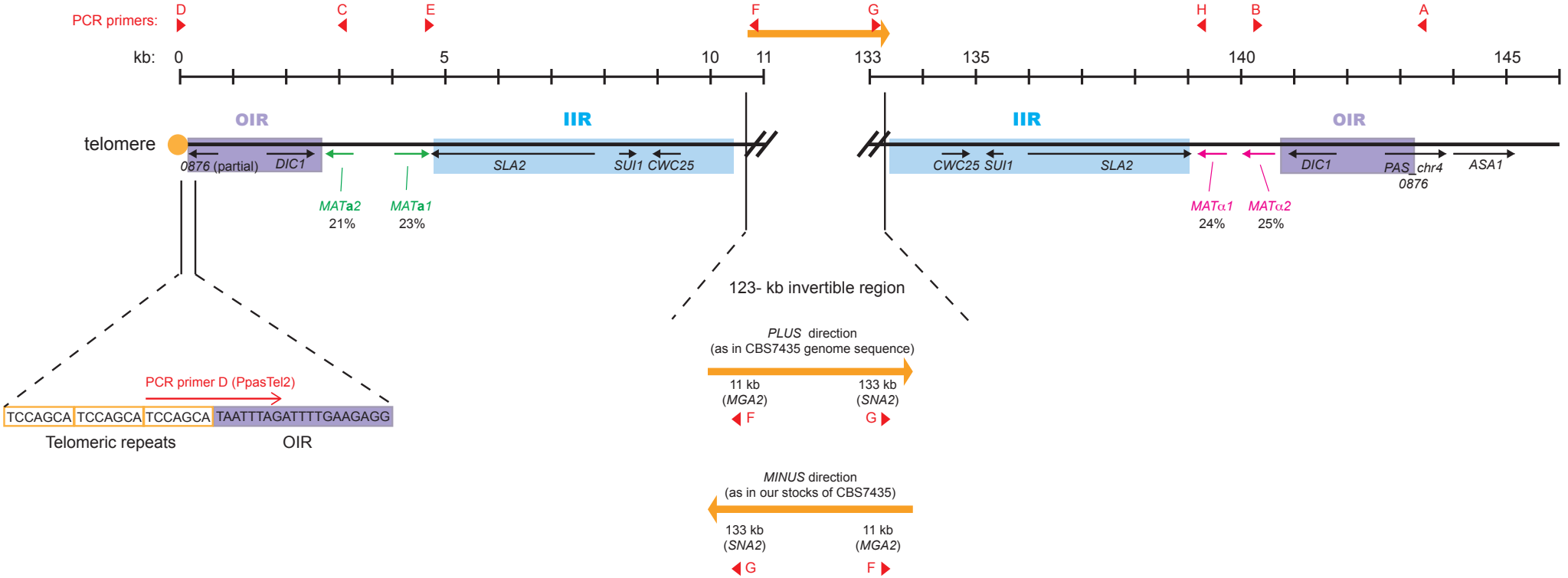

Hanson et al; Fig. S6

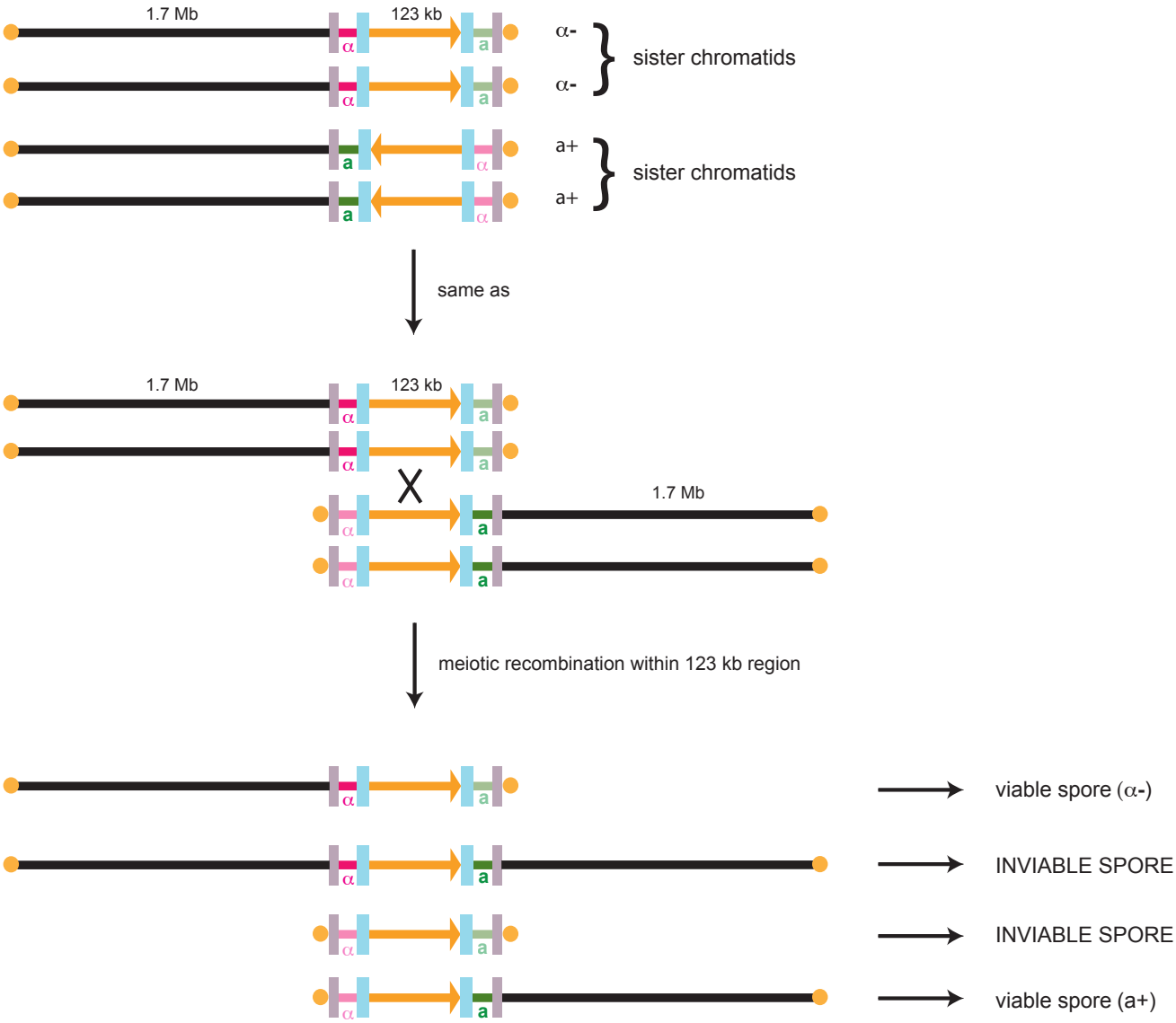

Hanson et al; Fig. S7

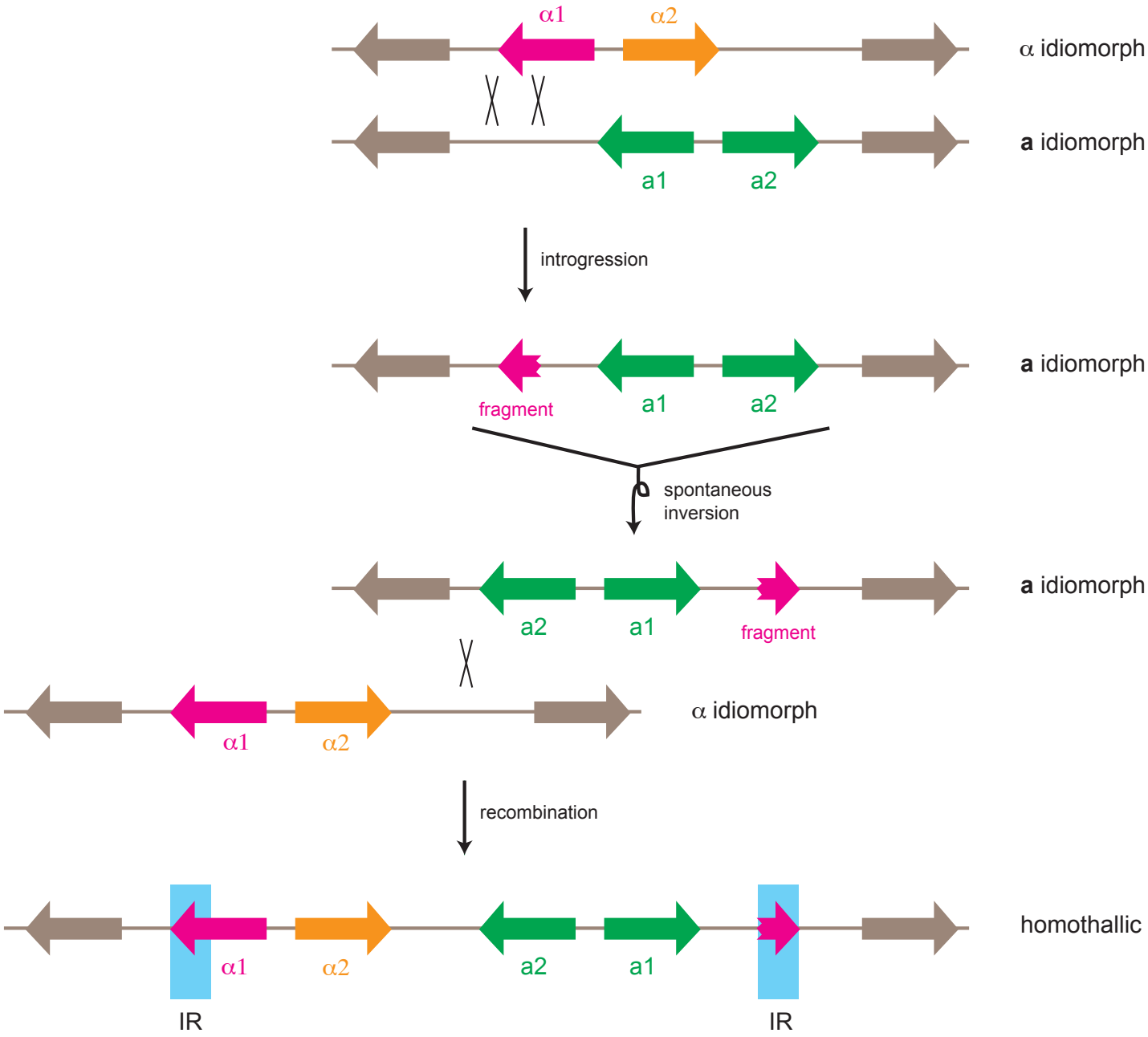

Hanson et al; Fig. S8

cccacacaccatagcttcaaaatgtttctactccttttttactcttccagattttctcggactccgcgcatcgccgtaccacttcaaaac
acccaagcacagcatactaaattttccctctttcttcctctagggtgtcgttaattacccgtactaaaggtttggaaaagaaaaaaga
gaccgcctcgtttctttttcttcgtcgaaaaaggcaataaaaatttttatcacgtttctttttcttgaaatttttttttttagttttttctctttcagtg
acctccattgatatttaagttaataaacggtcttcaatttctcaagtttcagtttcatttttcttgttctattacaacttttttacttcttgttcatta
gaaagaaagcatagcaatctaatctaaggggcgatggccaggttaaataagcacaagccggtgtcgacaacgccaaagac
gcccaagatgggctccagcacaagcttcaagaattcgccagccagtatcaagaaaacaccgtctaaatacccatacgatgttc
ctgactatgcgggctatccgtatgacgtcccggactatgcaggatcctatccatatgacgttccagattacgctagctctgagacgc
caaaggtcaaggcgggctcgacgttgagctctgggctcgcgagaaaccagccaggcgacccgacagaaatcaaaacgcag
aaaaaaagattcaagcccggaactgtggccttgcgcgagatcagaaggttccagaagtccacagagctgcttatcaggaaact
acccctttgctagactcgtcagagaaatcgtccaggacgagttcggaacaagcacctacagatggcagtcggtcgcagtgctggc
gttgcaggaagccgtcgaggcgtatcttgtgcatctttttgaggataccaacctgtgcgcgctccacgcgaagcgagtcaccatca
tgcagaaagacatccatcttgccaggagactgcgggggggattgaatcagtactgacaataaaaagattcttgttttcaagaacttg
tcatttgtatagttttttttatattgtagttgttctattttaatcaaatgttagcgtgatttatatttttttttcgcctcgacatcatctgcccagatgcg
aagttaagtgcgcagaaagtaatatcatgcgtcaatcgtatgtgaatgctggtcgctatactgctgtcgattcgatactaacgccgc
catccagtgtcgaaaac

Saccharomyces cerevisiae TEF1 promoter
Hansenula polymorpha CSE4
3xHA tag
Ashbya gossypii TEF1 terminator

Hanson et al; Fig. S9

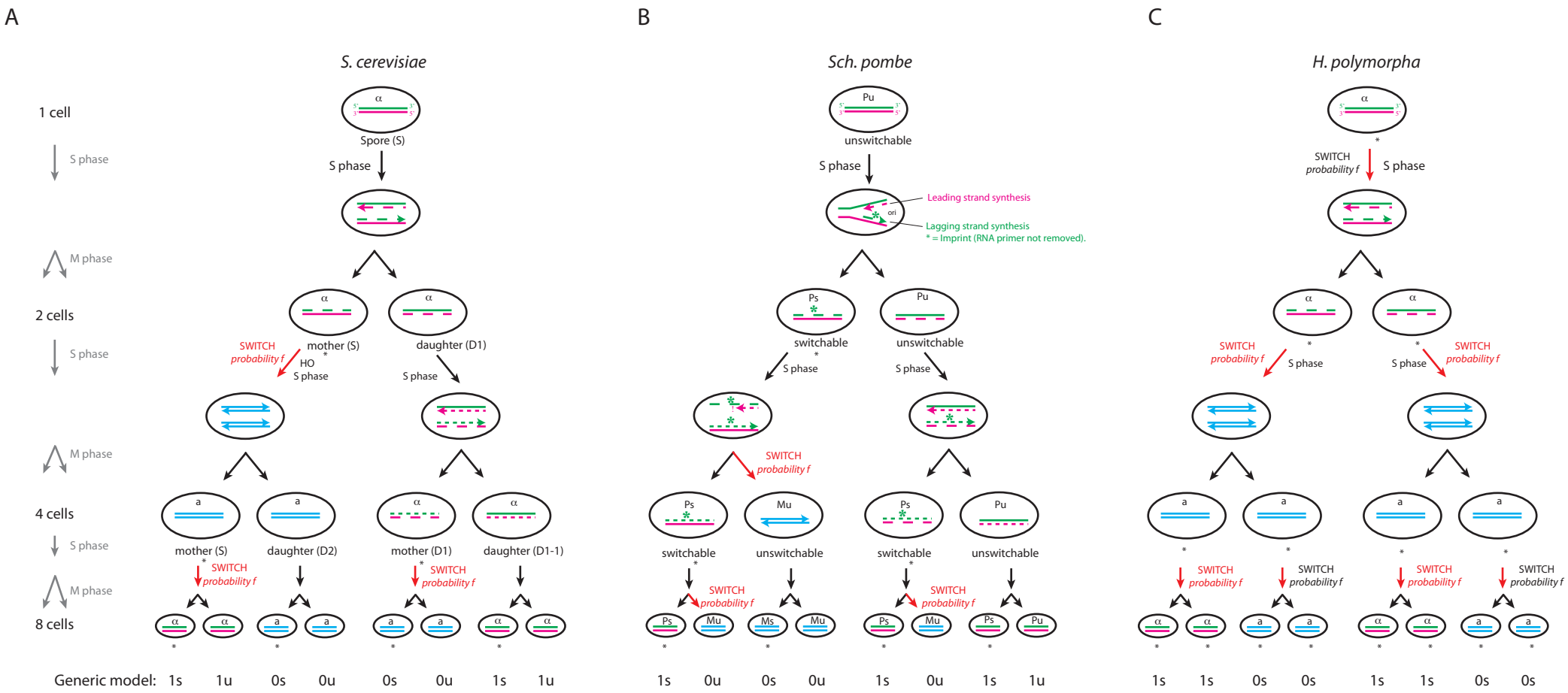

D

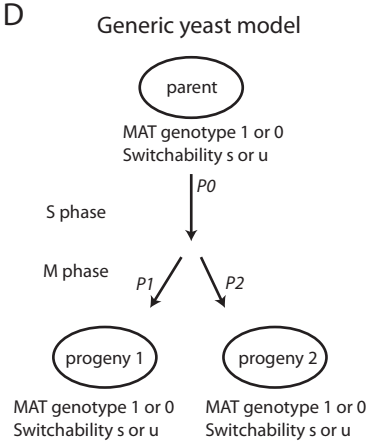

		S. cerevisiae parameters Switchability of parent	*Sch. pombe* parameters Switchability of parent	*H. polymorpha* parameters Switchability of parent
		s u	**s u**	**s u**
Probability of switching	*P0*	*f* 0	0 0	*f* N/A
	P1	0 0	0 0	0 N/A
	P2	0 0	*f* 0	0 N/A
Switchability of progeny	**progeny 1**	s	s	s
	progeny 2	u	u	s

Table S1. qRT-PCR of MAT loci in P. pastoris.

Gene	Strain	ACT1 Average C_T	a1 Average C_T	ΔC_T (a1-ACT1)	$\Delta\Delta C_T$ (GS190 vs. GS115)	**$a1_N$ relative to GS115**	$\Delta\Delta C_T$ (GS115 vs. SHY15)	$\Delta\Delta C_T$ (GS190 vs. SHY15)	**$a1_N$ relative to SHY15**
a1	GS115 (α)	22.40 ± 0.18	22.89 ± 0.14	0.49 ± 0.22	0.00 ± 0.22	**1.0 (0.85-1.16)**	-2.17 ± 0.22	----------	**4.50 (3.86-5.24)**
	GS190 (a)	22.99 ± 0.18	23.99 ± 0.34	0.91 ± 0.39	0.42 ± 0.39	**0.75 (0.57-0.97)**	----------	-1.75 ± 0.39	**3.36 (2.57-4.41)**
	SHY15 (α/a)	22.38 + 0.57	25.04 ± 0.73	2.66 ± 0.93	----------	----------	0.00 ± 0.93	0.00 ± 0.93	**1.0 (0.52-1.91)**
	Strain	ACT1 Average C_T	a2 Average C_T	ΔC_T (a2-ACT1)	$\Delta\Delta C_T$ (GS190 vs. GS115)	**$a2_N$ relative to GS115**	$\Delta\Delta C_T$ (GS115 vs. SHY15)	$\Delta\Delta C_T$ (GS190 vs. SHY15)	**$a2_N$ relative to SHY15**
a2	GS115 (α)	22.40 ± 0.18	28.41 ± 0.42	6.01 ± 0.46	0.00 ± 0.46	**1.0 (0.73-1.38)**	0.63 ± 0.46	----------	**0.65 (0.47-0.89)**
	GS190 (a)	22.99 ± 0.18	26.87 ± 0.31	3.88 ± 0.36	-2.13 ± 0.36	**4.38 (3.41-5.62)**	----------	-1.50 ± 0.36	**2.83 (2.20-3.63)**
	SHY15 (α/a)	22.38 + 0.57	27.76 ± 0.19	5.38 ± 0.60	----------	----------	0.00 ± 0.60	0.00 ± 0.60	**1.0 (0.66-1.52)**
	Strain	ACT1 Average C_T	α1 Average C_T	ΔC_T (α1-ACT1)	$\Delta\Delta C_T$ (GS115 vs. GS190)	**$\alpha1_N$ relative to GS190**	$\Delta\Delta C_T$ (GS115 vs. SHY15)	$\Delta\Delta C_T$ (GS190 vs. SHY15)	**$\alpha1_N$ relative to SHY15**
α1	GS115 (α)	22.40 ± 0.18	28.01 ± 0.14	5.60 ± 0.22	-0.86 ± 0.22	**1.82 (1.19-2.77)**	-0.26 ± 0.22	----------	**1.20 (1.03-1.39)**
	GS190 (a)	22.99 ± 0.18	29.46 ± 0.58	6.47 ± 0.61	0.00 ± 0.61	**1.0 (0.85-1.16)**	----------	0.61 ± 0.61	**0.66 (0.43-1.00)**
	SHY15 (α/a)	22.38 + 0.57	28.25 ± 1.25	5.86 ± 1.38	----------	----------	0.00 ± 1.38	0.00 ± 1.38	**1.0 (0.38-2.6)**
	Strain	ACT1 Average C_T	α2 Average C_T	ΔC_T (α2-ACT1)	$\Delta\Delta C_T$ (GS115 vs. GS190)	**$\alpha2_N$ relative to GS190**	$\Delta\Delta C_T$ (GS115 vs. SHY15)	$\Delta\Delta C_T$ (GS190 vs. SHY15)	**$\alpha2_N$ relative to SHY15**
α2	GS115 (α)	22.40 ± 0.18	26.92 ± 0.08	4.51 ± 0.19	-3.91 ± 0.19	**15.03 (13.18-17.15)**	-0.69 ± 0.19	----------	**1.61 (1.41-1.84)**
	GS190 (a)	22.99 ± 0.18	31.42 ± 0.86	8.43 ± 0.88	0.00 ± 0.88	**1.0 (0.54 -1.84)**	----------	3.23 ± 0.88	**0.11 (0.06-0.20)**
	SHY15 (α/a)	22.38 + 0.57	27.59 + 0.89	5.20 ± 1.06	----------	----------	0.00 ± 1.06	0.00 ± 1.06	**1.0 (0.48-2.08)**

$N = 2^{-\Delta\Delta CT}$; Values given + standard deviation

Table S2. Strains and plasmids used in this study.

Species	Strain name	Background	MAT locus designation (this study)	Genotype	Source
Hansenula polymorpha	CBS4732	CBS4732	MATalpha	*ade3 ura3*	Kantcho Lahtchev, Bulgarian Academy of Sciences, Sofia, Bulgaria
Hansenula polymorpha	DL-1	DL-1	MATalpha	*leu2 ura3*	Kantcho Lahtchev, Bulgarian Academy of Sciences, Sofia, Bulgaria
Hansenula polymorpha	NCYC495	NCYC495	MATa	*ade11 met6*	Kantcho Lahtchev, Bulgarian Academy of Sciences, Sofia, Bulgaria
Hansenula polymorpha	SH4330	NCYC495	MATalpha	*ura3*	Satoshi Harashima, Osaka University, Osaka, Japan
Hansenula polymorpha	SH4331	NCYC495	MATa	*ade11*	Satoshi Harashima, Osaka University, Osaka, Japan
Hansenula polymorpha	ura3	NCYC495	MATalpha	*ura3*	Ida van der Klei, University of Groningen, Groningen, Netherlands
Hansenula polymorpha	leu1.1	NCYC495	MATalpha	*leu1*	Ida van der Klei, University of Groningen, Groningen, Netherlands
Hansenula polymorpha	ade11.1	NCYC495	MATa	*ade11*	Ida van der Klei, University of Groningen, Groningen, Netherlands
Hansenula polymorpha	SHY2	NCYC495 X SH4330 (NCYC495)	MATa/alpha	*ade11/ADE11 met6/MET6 URA3/ura3*	This study
Hansenula polymorpha	SHY2-3	NCYC495 X SH4330 (NCYC495)	MATalpha	*ura3*	This study
Hansenula polymorpha	SHY2-4	NCYC495 X SH4330 (NCYC495)	MATa	*ura3*	This study
Hansenula polymorpha	SHY2-24	NCYC495 X SH4330 (NCYC495)	MATalpha	*met6*	This study
Hansenula polymorpha	SHY2-28	NCYC495 X SH4330 (NCYC495)	MATa	*met6*	This study
Hansenula polymorpha	SHY7	SHY2-3 X SHY2-24 (NCYC495)	MATa/alpha	*MET6/met6 ura3/URA3*	This study
Hansenula polymorpha	SHY10	SHY2-4 X SHY2-28 (NCYC495)	MATa/alpha	*MET6/met6 ura3/URA3*	This study
Hansenula polymorpha	SHY17	NCYC495	MATa	*ade11 met6 [pSH02]*	This study
Hansenula polymorpha	SHY32	NCYC495	MATalpha	*ura3 [pSH02]*	This study
Pichia pastoris	CBS7435	CBS7435	MATalpha-	WT	Spanish Type Culture Collection (CECT)
Pichia pastoris	GS115	CBS7435	MATalpha-	*his4*	Kristof De Schutter, Ghent University, Ghent, Belgium
Pichia pastoris	GS190	CBS7435	MATa+	*arg4*	James Cregg, Keck Graduate Institute of Applied Life Science, Claremont, CA
Pichia pastoris	JC254	CBS7435	MATalpha-	*ura3*	James Cregg, Keck Graduate Institute of Applied Life Science, Claremont, CA
Pichia pastoris	SHY14	GS115 X JC254 (CBS7435)	MATa+/alpha-	*HIS4/his4 ura3/URA3*	This study
Pichia pastoris	NRRL YB-378	NRRL YB-378	MATa-	WT	USDA Agricultural Research Service Culture Collection (from slime flux of elm tree, *Ulnus americana)*
Pichia pastoris	NRRL YB-4289	NRRL YB-4289	MATa-	WT	USDA Agricultural Research Service Culture Collection (from black oak tree *Quercus kelloggii*)
Pichia pastoris	NRRL Y-7556	NRRL Y-7556	MATa+	WT	USDA Agricultural Research Service Culture Collection (from black oak tree *Quercus kelloggii*)
Pichia pastoris	NRRL Y-12729	NRRL Y-12729	MATalpha-	WT	USDA Agricultural Research Service Culture Collection (unknown habitat)
Pichia pastoris	NRRL Y-17741	NRRL Y-17741	MATalpha+	WT	USDA Agricultural Research Service Culture Collection (from sap flux of Emory oak tree, *Quercus emoryi*)
Plasmid	pSH02	pRS406	N/A	panARS - KanMX - pScTEF-3HA-HpCSE4	This study

Table S3. Primers used in this study.

Primer name	sequence (5'-3')	Label in figure
MAT locus PCR		
HpolMATa2	CCACTCATGGGAAATGATCCG	A
HpolMATb1	GAGTCATGGGGTCTGGTTTG	B
HpolMATb2	CTGCATGATATGACTACCAGCC	B
HpolMATc1	CTCAGATGATCCCACCACTAGG	C
HpolMATd1	CTGCGTCAGCTCAGGAATC	D
PpasAlpha2_1	GAGAGTTTTCTTTGGGAGGAGC	B
PpasA2_1	GGCATAACCACGCAGGATATC	C
PpasMFS_1	CCCAGGTAAGTCAAAGCTGC	A
PpasMFS_2	GTTTGAGATTGAGGCCCAGCATAG	A
PpasTel_1	TCCAGCATCCAGCATCCAGCA	D
PpasTel_2	TCCAGCATCCAGCATAATTTAGA	D
PpInt_E1	CTTCAAGCTCAGTCCCATCC	E
PpInt_F1	CGTGGTGCTATCAGCTAATGTGCC	F
PpInt_G1	GTGCGACTCTCCACTAGAGC	G
PpInt_H1	CCTGGAATGAGCTACTCAGC	H
RT-PCR		
Hpola1-2	CACTCTTTGTAGACGTCCAGTTC	
HpolMATb2	CTGCATGATATGACTACCAGCC	
Hpola2-1	ATCAGTGAAGGGCGTAGCAAAC	
Hpola2-2	GCGGCCAACTGGATTTTAGGTC	
Hpolalpha2-1	GGTTAGTGTTCGCTCCTTTCTTC	
Hpolalpha2-2	GAACGTCAAATACGAGCAGCCAG	
Hpolalpha1-1	GCATTCCTGAAATACATCCTCGAC	
HpolMATc2	CCATTCAAAGAGCAAGGAACCG	alpha1
HpGAPDHF1	GGAAGAATTGGTAGACTGGTGTTG	
HpGAPDHR1	GTTCCCTTGAACTTTCCGTGTG	
PpA1F1	CCAAGCTCTCACTTATCGACTGC	
PpA1R1	CGAGATGACTGACGGGTCA	
PpA2F3	CGAGTACCTGCAAATCGAGG	
PpA2R1	GGTTTACGGTTCTCCTGCG	
PpAlpha1F3	ACTGGTGAAAATCAATACAGCGA	
PpAlpha1R1	CCATGCGACAGATAATAGTCTCG	
PpAlpha2F2	GCAAGGGATATCTCATAATGCG	
Ppalpha2_2	CACGTCGTTCTTGAGCATTCTC	
PpGAPDHF1	CCCACAAGGCTTACAAGGGT	
PpGAPDHR1	ACACCGGTGGACTCAATGAC	
PpTUB1F3	CCAACTTGGTTCCATACCCA	
PpTUB1R1	CACACTTGACCATTTGGTTGCTG	
PpACT1F1	ACACAGTGTTCCCATCGGTC	
PpACT1R1	ACCGTGCTCGATTGGGTATC	
ChIP qPCR		
Hp_regB2F	CTTGGAAAACTTACTGCTGGGTAG	899 kb
Hp_regB1R	TGCCCGTGAGAATGGGATC	899 kb
Hp_Tpa5ds_3F	GGCCAACCGAACCACTTCTATTTC	898 kb
Hp_Tpa5ds_2R	TTCGTCCCAATTCCAGGATAAC	898 kb
Hp alpha1-2	CCAACTACGTCGCCCTTAC	
Hp alpha1-3	GCCATGAAACCATTCAAACGC	
Hpolalpha2-2	GAACGTCAAATACGAGCAGCCAG	
Hp_alpha2-3	CGGTAGTGAAACCTTCCATTGAAG	
HpolMATb2	CTGCATGATATGACTACCAGCC	
Hp_a1-4	TCCAAGATCCTCACGCCTTC	
Hp a2-2	GCGGCCAACTGGATTTTAGGTC	
Hp a2-1	ATCAGTGAAGGGCGTAGCAAAC	
HpDIC1_1	GCATGCATTGGATGGCTTAC	
HpDIC1_2	CATGAATCCCAAGCCTTCTCTAG	
Hp FAS2_1	GGCGCCTTACACAGATGAC	
Hp FAS2_3	GCATCTCAGCTGTTTCTGTCG	
Hp ORF_1	GGCATTTGTTGTTAGTTCACACC	
Hp ORF_2	CCATATGAAAGTCGATGCCGTC	
Hp_GAPDHF1	GGAAGAATTGGTAGACTGGTGTTG	
Hp_GAPDHR1	GTTCCCTTGAACTTTCCGTGTG	